

# Quantile Mediation Analytics

BY CANYI CHEN

*Department of Biostatistics, University of Michigan,  
Ann Arbor, Michigan 48104, U.S.A.  
canyic@umich.edu*

YINQIU HE

*Department of Statistics, University of Wisconsin,  
Madison, Wisconsin 53706, U.S.A.  
yinqiu.he@wisc.edu*

HUIXIA J. WANG

*Department of Statistics, George Washington University,  
Washington, DC 20052, U.S.A.  
judywang@email.gwu.edu*

GONGJUN XU

*Department of Statistics, University of Michigan,  
Ann Arbor, Michigan 48104, U.S.A.  
gongjun@umich.edu*

AND PETER X.-K. SONG

*Department of Biostatistics, University of Michigan,  
Ann Arbor, Michigan 48104, U.S.A.  
pxsong@umich.edu*

## SUMMARY

Mediation analytics help examine if and how an intermediate variable mediates the influence of an exposure variable on an outcome of interest. Quantiles, rather than the mean, of an outcome are scientifically relevant to the comparison among specific subgroups in practical studies. Albeit some empirical studies available in the literature, there lacks a thorough theoretical investigation of quantile-based mediation analysis, which hinders practitioners from using such methods to answer important scientific questions. To address this significant technical gap, in this paper, we develop a quantile mediation analysis methodology to facilitate the identification, estimation, and testing of quantile mediation effects under a hypothesized directed acyclic graph. We establish two key estimands, quantile natural direct effect (qNDE) and quantile natural indirect effect (qNIE), in the counterfactual framework, both of which have closed-form expressions. To overcome the issue that the null hypothesis of no mediation effect is composite, we establish a powerful adaptive bootstrap method that is shown theoretically and numerically to achieve a proper type I error control. We illustrate the proposed quantile mediation analysis methodology through both extensive simulation experiments and a real-world dataset in that we investigate the mediation

effect of lipidomic biomarkers for the influence of exposure to phthalates on early childhood obesity clinically diagnosed by 95<sup>th</sup> percentile of body mass index.

*Some key words:* Adaptive bootstrap; causal estimand; composite null hypothesis; Gaussian copula; generalized structural equation model.

## 1. INTRODUCTION

Mediation analysis is one of the effective statistical methodologies to learn and infer structural parameters in a certain pathway of scientific importance. It enables practitioners to determine if, and to what extent, one or many immediate variables mediate the influence of exposures, either environmental or social, on outcomes of interest under hypothesized prespecified directed acyclic graphs (DAGs); see, for example, Sobel (1982) and Baron & Kenny (1986). To date, mediation analysis has been extensively applied in practice, such as psychology, genomics and epidemiology (Guo et al., 2022), just name a few.

Most existing theories, methods, and applications of mediation analysis have concerned the mean of an outcome with few results available in the quantile regression paradigm. However, studying quantiles is crucial as they offer a unique perspective for examining the data-generation distribution, addressing important scientific questions that the mean alone may not fully capture. For example, in studies of childhood obesity, children aged two or older are clinically diagnosed as obese if their body mass index (BMI) falls at or above the 95th percentile for their age (Centers for Disease Control and Prevention, 2022). In aging studies, an individual with their biological age surpassing the population median is deemed as accelerated aging, a stage of evolution linked to elevated risk of diseases onset such as Alzheimer’s, diabetes and cancers (Horvath, 2013).

Three significant technical challenges arise when quantiles, rather than the mean, of an outcome are of interest in mediation analyses. First, the continuity of the variables disqualifies existing stratification-based methods proposed by Huber et al. (2022) while discretization approaches (Hsu et al., 2023) may suffer from approximation errors and/or excessive computational costs in large-scale applications. Second, in comparison with the linear mean model, the nonlinearity of the quantile regression introduces inherent complexity to establish identifiability conditions for causal effects, resulting in a paucity of literature offering interpretable expressions for quantile mediation effects (Shen et al., 2014; Yuan & MacKinnon, 2014; Bind et al., 2017). Third, partly arising from the first two, involves the development of valid hypothesis testing procedures. As we will demonstrate in Section 3, since the null hypothesis of no quantile mediation effect appears composite, the limiting null distributions are found to vary across different subspaces of the null hypothesis. Consequently, conservative control of type I error prevails in almost all existing tests, including popular generalized Sobel’s test and MaxP test as well as the classical bootstrap procedure (Sobel, 1982; Yuan & MacKinnon, 2014; Wang & Yu, 2023). Such conservatism is illustrated by both simulation studies and data applications in Sections 4 and 5.

In this paper, we propose an important extension of generalized structural equation models (Hao et al., 2023, SEM) to set up a unified framework for evaluating quantile mediation effects in the presence of continuous exposure, mediator and outcome variables. Through such a new framework, we can write key quantile mediation estimands in closed-form expressions so that analyzing and interpreting quantile mediation effects becomes conceptually straightforward and computationally easy. In addition, we introduce a valid hypothesis testing procedure based on an adaptive bootstrap (AB) to test the null hypothesis of no quantile mediation effect. Our AB test leverages the explicit derivation of the limiting null distribution under the composite null, followed by a pretest to distinguish among different null hypotheses prior to conducting the

bootstrap. The consistency of the bootstrap procedure under both the null and a local alternative ensures valid Type I error control with enhanced statistical power.

Of note, the generalized SEM is originally proposed to analyze mean mediation effects in non-Gaussian data, using hierarchical modeling and Gaussian copula to construct the joint distribution. An advantage of employing Gaussian copula in the construction of DAG stems from the motivation of preserving causal topology in a similar spirit to the classical linear SEM (Hao et al., 2023; Wang et al., 2018a; Zhou et al., 2021). Refer to a further discussion of the DAG topology preservation in Appendix A, where the causal pathway is exclusively characterized by the second moments of the joint distribution while confounding variables affect only the first moments of the joint distribution (Frisch & Waugh, 1933). In such constructed DAG, quantiles naturally hedge with rank-based correlations for easy interpretation. Furthermore, because of such separability between DAG topology and confounding adjustment, the resulting quantile mediation analytics appear to be rather resilient to complex data structures and lead to interpretable results of practical relevance. Moreover, the model diagnostics are readily available to check specific model assumptions (Zhang et al., 2016) in addition to conventional sensitivity analyses.

This paper is organized as follows. Section 2 introduces the generalized SEM, followed by the derivation of key quantile mediation estimands, where more details of the generalized SEM are relegated to Appendix A. Section 3 concerns the development of adaptive bootstrap procedures for hypothesis testing of composite nulls. Sections 4 and 5 focus on evaluating the performance of the proposed methodology through, respectively, extensive simulation experiments and a real data application. Concluding remarks are included in Section 6. All technical proofs are relegated to the online Supplementary Material.

## 2. QUANTILE MEDIATION EFFECT

We begin with the generalized SEM, a joint distribution of exposure  $S \in \mathbb{R}$ , mediator  $M \in \mathbb{R}$ , outcome  $Y \in \mathbb{R}$  conditional on the  $p$ -element vector of confounders  $X \in \mathbb{R}^p$  given by

$$F_{S,M,Y|X}(s, m, y | x) = C\{F_{S|X}(s | x), F_{M|X}(m | x), F_{Y|X}(y | x); \Gamma'\}, \quad (2.1)$$

where  $C$  is a Gaussian copula (Song, 2000), and the dependence matrix  $\Gamma'$  is given in (A.1); see Appendix A for more details. Such specified joint distribution  $F_{S,M,Y|X}(s, m, y | x)$  incorporates generalized linear models (GLMs) in the marginal distributions, respectively. According to Hao et al. (2023), this construction preserves the DAG topology shown in Figure 1 (B) with two key pathways, namely  $S \rightarrow Y$  and  $S \rightarrow M \rightarrow Y$ . In classical linear SEM, the former pathway refers to a direct effect  $\gamma_S$ , while the latter is known as the mediation pathway with effect size  $\alpha_S \beta_M$ . These effects become more complicated in the generalized SEM in connection to quantiles, which will be studied in detail in this paper. This joint distribution can produce conditional distributions, marginal distributions, and, more importantly, quantile functions as desired for the study of quantile mediation effects.

### 2.1. Definition of Quantile Causal Effects

Given a quantile level  $\tau \in (0, 1)$  and random variables  $S$  and  $Y$ ,  $Q_Y(\tau) \stackrel{\text{def}}{=} \inf\{y \in \mathbb{R} : \text{pr}(Y \leq y) \geq \tau\}$  denotes its  $\tau$ -th marginal quantile of  $Y$ , and  $Q_{Y|S}(\tau | s) \stackrel{\text{def}}{=} \inf\{y \in \mathbb{R} : \text{pr}(Y \leq y | S = s) \geq \tau\}$  denotes the  $\tau$ -th conditional quantile of  $Y$  on variable  $S = s$ . In the following,  $Q_{Y|S}(\tau | s)$  is abbreviated as  $Q_{Y|S}(\tau)$  when there is no ambiguity.

To proceed with the counterfactual paradigm, let  $M(s)$  represent a potential value of the mediator  $M$  when exposure  $S = s$ , and let  $Y(s, m)$  represent a potential outcome when exposure

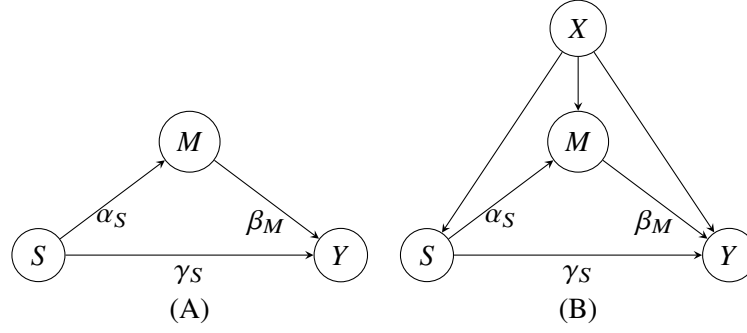


Fig. 1: Directed acyclic graphs for unconfounded and confounded mediation models in (A) and (B), respectively.  $S$ : exposure,  $M$ : mediator,  $Y$ : outcome,  $X$ : confounders;  $\alpha_S, \beta_M, \gamma_S$ : structural coefficients.

$S = s$  and mediator  $M = m$ . We assume the Stable Unit Treatment Value assumption (SUTV, Rubin, 1980):

*Condition 1 (Stable Unit Treatment Value Assumption).*  $M = M(S)$ , and  $Y = Y(S, M(S))$ .

Given two exposures levels  $s$  and  $s'$ , the conditional quantile natural direct effect (qNDE) at the  $\tau$ -th quantile level is defined as,

$$\text{qNDE}_\tau(s, s'; x) \stackrel{\text{def}}{=} Q_{Y(s', M(s))|X}(\tau | x) - Q_{Y(s, M(s))|X}(\tau | x). \quad (2.2)$$

Likewise, the conditional quantile natural indirect effect (qNIE) at the  $\tau$ -th quantile level is defined as

$$\text{qNIE}_\tau(s, s'; x) \stackrel{\text{def}}{=} Q_{Y(s', M(s'))|X}(\tau | x) - Q_{Y(s', M(s))|X}(\tau | x). \quad (2.3)$$

It follows that a sum of qNDE and qNIE gives the conditional quantile total effect (qTE) at the  $\tau$ -th quantile level:

$$\text{qTE}_\tau(s, s'; x) \stackrel{\text{def}}{=} \text{qNIE}_\tau(s, s'; x) + \text{qNDE}_\tau(s, s'; x) = Q_{Y(s', M(s'))|X}(\tau | x) - Q_{Y(s, M(s))|X}(\tau | x).$$

This  $\text{qTE}_\tau$  is similar to the  $\eta = \alpha_S \beta_M + \gamma_S$  in the classical SEM introduced in Appendix A, and summarizes all causal impacts on  $Y$  at the  $\tau$ -th quantile level due to  $S$ .

The above definitions of conditional qNDE and qNIE present a substantial extension of the conditional quantile total effect discussed in Li et al. (2023), with the inclusion of a mediator and associated pathways. The adoption of the copula hierarchical modeling approach provides two key technical advantages. First, it significantly simplifies the estimation procedure as the DAG parameters and effects of confounding factors can be separately estimated, thereby greatly lowering computational demands. Second, it can improve estimation efficiency and statistical power in the inference for qNDE and qNIE by minimizing the disturbance from confounders. Moreover, both qNDE and qNIE defined under the unified framework of generalized SEM give attractive interpretability comparable to that of their counterparts in the classical linear SEM. Thus, our methodology covers many important models that have been studied separately in the literature, including VanderWeele & Vansteelandt (2010) examining conditional odds ratios, and Bind et al. (2017) exploring conditional controlled effects in the context of longitudinal data.

## 2.2. Identifiability

We now present sufficient conditions for the identification of causal quantile mediation effect  $S \rightarrow M \rightarrow Y$  as shown in Figure 1 under the counterfactual framework (VanderWeele, 2015).

These conditions are widely utilized in the causal inference literature to ensure that the causal effect can be expressed as a function of observable quantities. One key theoretical advantage is that under the assumption of *Sequential Ignorability* (SI, Imai et al., 2010b; Shpitser & VanderWeele, 2011), the generalized SEM provides closed-form expressions for both  $\text{qNIE}_\tau(s, s'; x)$  and  $\text{qNDE}_\tau(s, s'; x)$ , which brings not only technical convenience and numerical ease but also interpretability in practice.

*Condition 2 (Sequential Ignorability Assumption).* For all levels of  $s, s', m$  and  $x$ , the potential outcomes generated by the generalized SEM satisfy: (i)  $\{Y(s, m), M(s')\} \perp\!\!\!\perp S \mid X = x$ ; and (ii)  $Y(s, m) \perp\!\!\!\perp M(s') \mid \{S = s', X = x\}$ .

Here  $A \perp\!\!\!\perp B \mid C$  denotes the conditional independence of  $A$  and  $B$  on  $C$ . Condition 2 (i) states that given confounders  $X$ , exposure  $S$  is independent of the potential outcome  $Y(s, m)$  and the potential mediator  $M(s')$ . Condition 2 (ii) requires that the potential outcome  $Y(s, m)$  and the mediator  $M$  are independent conditional on  $S$  and  $X$ . Under the above identifiability conditions, both  $\text{qNDE}$  and  $\text{qNIE}$  can be written as closed-form expressions in Theorem 1 below. For any value  $s$  of  $S$ , denote the normal score by  $z_s \equiv z_s(x) \stackrel{\text{def}}{=} \Phi^{-1}\{F_{S|X}(s \mid x)\}$ , and let  $\delta_Y = (\eta^2 + \beta_M^2 + 1)^{1/2}$  with  $\eta = \alpha_S \beta_M + \gamma_S$ .

**THEOREM 1.** For continuous  $S, M$  and  $Y$ , under Conditions 1 and 2, the closed-form expressions of  $\text{qNIE}_\tau(s, s'; x)$  and  $\text{qNDE}_\tau(s, s'; x)$  are given by, respectively,

$$\begin{aligned} \text{qNDE}_\tau(s, s'; x) &= Q_{Y|X}\{\Phi(\Delta_{s',s}(\tau)) \mid x\} - Q_{Y|X}\{\Phi(\Delta_{s,s}(\tau)) \mid x\}, \text{ and} \\ \text{qNIE}_\tau(s, s'; x) &= Q_{Y|X}\{\Phi(\Delta_{s',s'}(\tau)) \mid x\} - Q_{Y|X}\{\Phi(\Delta_{s',s}(\tau)) \mid x\}, \end{aligned}$$

where  $\Delta_{s',s}(\tau) \equiv \Delta_{s',s}(x; \tau) \stackrel{\text{def}}{=} \{\gamma_S z_{s'} + \alpha_S \beta_M z_s + \Phi^{-1}(\tau)(1 + \beta_M^2)^{1/2}\} / \delta_Y$  and other terms are similarly defined. Moreover, we have (i)  $\text{qNDE}_\tau(s, s'; x) = 0$  if and only if  $\gamma_S = 0$ ; and (ii)  $\text{qNIE}_\tau(s, s'; x) = 0$  if and only if  $\alpha_S \beta_M = 0$ .

The term  $\Delta_{s',s}(\tau)$  plays a pivotal role in both  $\text{qNDE}_\tau(s, s'; x)$  and  $\text{qNIE}_\tau(s, s'; x)$ , which is comprised of two components. One is the constant base component,  $(\gamma_S z_{s'} + \alpha_S \beta_M z_s) / \delta_Y$ , which is independent of quantile level  $\tau$ , and the other is “drift” component depending multiplicatively on the  $\tau$ -th normal quantile,  $\Phi^{-1}(\tau)(1 + \beta_M^2)^{1/2} / \delta_Y$ . The base component is driven by the exposure levels  $s$  and  $s'$  along with the strengths of two pathways  $(\alpha_S \beta_M, \gamma_S)$ . In contrast, the drift is proportionally modified by the  $\tau$ -level normal quantile on  $\{1 - \eta^2 / (\eta^2 + \beta_M^2 + 1)\}^{1/2} = [1 - \text{corr}^2\{z_S(x), z_Y(x)\}]^{1/2}$ , which may be regarded as “the unexplained effect by  $S$ ” for outcome  $Y$  with the generalized SEM approach to model the DAG. While this decomposition shares similarities with the quantiles of the Gaussian distribution, the non-linear rank transformation  $\Phi^{-1}F_{S|X}(\cdot \mid x)$  allows our framework to accommodate more general data types.

Theorem 1 depicts profiles of  $\text{qNIE}$  and  $\text{qNDE}$  across different quantile levels for many concrete examples. Below we exemplify Theorem 1 with two particular examples.

*Example 1.* When  $S$  and  $Y$  given  $X = x$  are normally distributed,  $S \mid X = x \sim \mathcal{N}(\mu_S(x), \sigma_S^2)$  and  $Y \mid X = x \sim \mathcal{N}(\mu_Y(x), \sigma_Y^2)$ , it is easy to show that the  $\text{qNDE}_\tau$  and  $\text{qNIE}_\tau$  are given by

$$\text{qNDE}_\tau(s, s'; x) = \frac{\sigma_Y}{\sigma_S \delta_Y} \gamma_S (s' - s), \text{ and } \text{qNIE}_\tau(s, s'; x) = \frac{\sigma_Y}{\sigma_S \delta_Y} \alpha_S \beta_M (s' - s).$$

This example is trivial in the sense that both estimands are independent of quantile level  $\tau$  and in fact coincide with their mean counterparts given in Hao et al. (2023). The normal quantile term  $\Phi^{-1}(\tau)$  is canceled out in calculation of the  $\text{qNDE}$  and  $\text{qNIE}$ .

Such cancellation disappears in many cases. The following example, motivated by our childhood obesity metabolic study in Section 5, illustrates a nontrivial application of qNDE and qNIE.

*Example 2.* For simplicity, we consider a special scenario where the  $\text{qNDE}_\tau(s, s'; x)$  is zero, but the  $\text{qNIE}_\tau(s, s'; x)$  varies over  $\tau$ , and  $X \equiv 1$  (no confounding). Suppose that marginally  $S \sim \mathcal{N}(0, 1)$ ,  $M \sim \mathcal{N}(0, 1)$  and  $Y \sim \text{Exp}(1)$ , and the joint distribution of  $(S, M, Y)$  is given by the generalized SEM via the Gaussian copula. Set  $(\alpha_S, \beta_M, \gamma_S) = (1, 1, 0)$ . Consider a change from  $s = 0$  to  $s' = 1$ . We plot  $\text{qNDE}_\tau(s, s'; x)$  and  $\text{qNIE}_\tau(s, s'; x)$  over  $\tau$ , respectively, in Figure 2 (A) and (B). The plot of qNDE is flat because we intentionally set  $\gamma_S = 0$ , and the plot of  $\text{qNIE}_\tau(s, s'; x)$  is an increasing function in  $\tau$  under  $\alpha_S \beta_M \neq 0$ , confirming the if-and-only-if result in Theorem 1.

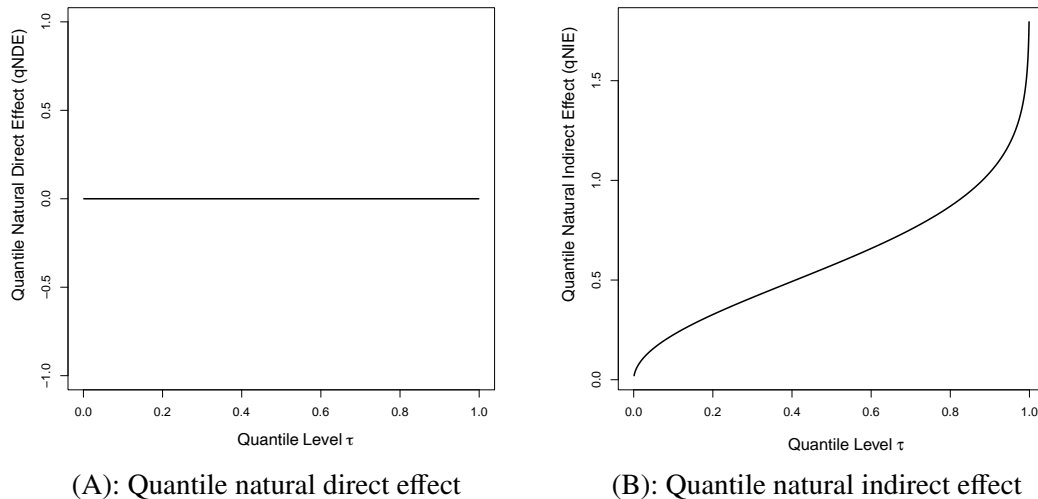


Fig. 2: Plots of the qNDE in (A) and qNIE in (B) under a generalized SEM with  $X \sim \mathcal{N}(0, 1)$ ,  $M \sim \mathcal{N}(0, 1)$  and  $Y \sim \text{Exp}(1)$ . The DAG model parameters  $(\alpha_S, \beta_M, \gamma_S)$  are set so that qNDE equals to zero (constant) while qNIE varies over quantile level  $\tau$  when exposure changes from  $s = 0$  to  $s' = 1$ .

### 2.3. Analytic Tasks

One primary task pertains to parameter estimation. Given that the generalized SEM is fully parametric, the maximum likelihood estimation (MLE) is a natural choice of the method for parameter estimation. With the availability of likelihood, we can directly estimate  $\text{qNIE}_\tau(s, s'; x)$  and  $\text{qNDE}_\tau(s, s'; x)$  by plugging in the MLEs of the model parameters. This is because both  $\widehat{Q}_{Y|X}(\cdot)$  and  $\widehat{F}_{S|X}(\cdot)$  are obtained as the plug-in estimates for  $Q_{Y|X}(\cdot)$  and  $F_{S|X}(\cdot)$ , respectively. See the details in Section C of the Supplementary Material.

In the implementation of MLE, we adopt the widely used strategy proposed by Joe (2005) in the literature of copula dependence models. The so-called Inference Function with Marginals (IFM) is known to be computationally efficient to handle nuisance parameters in the marginals. Specifically, given a random sample  $\{(S_i, M_i, Y_i, X_i)\}_{i=1}^n$  of size  $n$ , we run MLE to obtain the estimates of the model parameters  $(\widehat{\alpha}_S, \widehat{\beta}_M, \widehat{\gamma}_S, \widehat{\zeta}_S^\tau, \widehat{\zeta}_M^\tau, \widehat{\zeta}_Y^\tau, \widehat{\phi}_S, \widehat{\phi}_M, \widehat{\phi}_Y)$  where the DAG parameter estimates  $(\widehat{\alpha}_S, \widehat{\beta}_M, \widehat{\gamma}_S)$  are calculated after the marginal model parameter estimates

$(\widehat{\zeta}_S^\tau, \widehat{\zeta}_M^\tau, \widehat{\zeta}_Y^\tau, \widehat{\phi}_S, \widehat{\phi}_M, \widehat{\phi}_Y)$  are obtained. As shown by Joe (2005), IFM produces asymptotically efficient MLE.

Another primary task in the mediation analysis is to establish mediation pathways. To do so, for given  $\tau$ ,  $s$ ,  $s'$  and  $x$ , we plan to perform a hypothesis testing of the form:

$$H_0: \text{qNIE}_\tau(s, s'; x) = 0 \text{ versus } H_1: \text{qNIE}_\tau(s, s'; x) \neq 0. \quad (2.4)$$

Here, we focus on a single quantile level at each test, which is the most basic test considered in practice. In our motivating example with the outcome of child's BMI, we are interested in the quantile level  $\tau = 0.95$  that corresponds to the clinical definition of childhood obesity.

According to Theorem 1, the null hypothesis  $H_0: \text{qNIE}_\tau(s, s'; x) = 0$  is equivalent to  $\alpha_S \beta_M = 0$ . Under this null hypothesis, the DAG parameters  $(\alpha_S, \beta_M)$  control all quantile profiles. In contrast, under the alternative hypothesis, the  $\text{qNIE}_\tau$  can vary with different quantile levels  $\tau$ . However, this hypothesis test is nontrivial due to a composite null hypothesis. That is, the underlying null parameter space  $\Omega_0 = \{(\alpha_S, \beta_M) : \alpha_S \beta_M = 0\}$  constitutes three subspaces:

$$\begin{aligned} \Omega_{0,1} &= \{(\alpha_S, \beta_M) : \alpha_S = 0, \beta_M \neq 0\}, & \Omega_{0,2} &= \{(\alpha_S, \beta_M) : \alpha_S \neq 0, \beta_M = 0\}, \\ \Omega_{0,3} &= \{(\alpha_S, \beta_M) : \alpha_S = 0, \beta_M = 0\}. \end{aligned}$$

Such a composite null, especially the singleton  $\Omega_{0,3}$ , poses significant technical difficulties in the development of valid testing procedures. The existing popular approaches to testing the null (2.4) include Wald-type tests and classic nonparametric bootstrap methods. However, neither methods can control type I error properly; see our extensive numerical studies in Section 4. Under singleton  $\Omega_{0,3}$ , limiting behaviors of existing statistics become analytically irregular. Proposition 1 provides a rigorous theoretical justification for such irregularity. Proposition 1 implies that the usual first-order delta method fails to deliver the legitimate limiting null distribution for (2.4) under  $\Omega_{0,3}$ , whereas under  $\Omega_{0,1}$  and  $\Omega_{0,2}$ , such delta method works to establish a valid Wald-type test for  $\text{qNIE}_\tau(s, s'; x)$ . This is because the limiting distribution of  $\widehat{\text{qNIE}}_\tau(s, s'; x)$  varies under different null subspaces, resulting in an irregularity issue.

**PROPOSITION 1.** *Under the conditions of Theorem 1, the irregularity issue exists under the null hypothesis  $H_0$ , that is*

$$\begin{aligned} (i) \quad & \nabla_{\alpha_S} \text{qNIE}_\tau(s, s'; x) \Big|_{\beta_M=0} = \nabla_{\beta_M} \text{qNIE}_\tau(s, s'; x) \Big|_{\alpha_S=0} = 0, \\ (ii) \quad & \nabla_{\alpha_S} \text{qNIE}_\tau(s, s'; x) \Big|_{\alpha_S=0, \beta_M \neq 0} \neq 0, \quad (iii) \quad \nabla_{\beta_M} \text{qNIE}_\tau(s, s'; x) \Big|_{\alpha_S \neq 0, \beta_M=0} \neq 0. \end{aligned}$$

This issue has been noticed on other occasions, such as three-way contingency table analysis and factor analysis; see, for example, Glonek (1993), Dufour et al. (2013), and Drton & Xiao (2016). In particular, Wang & Yu (2023) pointed out that under the linear quantile mediation analysis, the composite null structure further worsens the type I error control given that the underlying true situation is unknown.

### 3. ADAPTIVE BOOTSTRAP TEST

The recent solution based on an adaptive bootstrap (AB) test by He et al. (2023) in the linear SEM shed light to handle the singleton  $\Omega_{0,3}$ . In this section, we extended the AB test to the case of quantile mediation analysis to test the null hypothesis (2.4) with a proper type I error control. We begin with some notations. Given two sequences of real numbers  $\{a_n\}$  and  $\{b_n\}$ , write  $a_n = o(b_n)$  if  $a_n/b_n \rightarrow 0$ . Convergence in distribution is denoted by  $\xrightarrow{d}$ , while  $\xrightarrow{d^*}$

denotes bootstrap consistency with respect to the Kolmogorov-Smirnov distance (Section 23.2, van der Vaart, 1998). More details about these convergence modes are listed in Section A of the Supplementary Material.

### 3.1. Formulation

The key idea of the AB approach is rooted in a local asymptotic analysis framework to address the irregularity round  $(\alpha_S, \beta_M) = (0, 0)$  and to examine the asymptotic behaviors of  $\widehat{\text{qNIE}}_\tau(s, s'; x)$  under local alternatives. That is, we explore limiting distributions with parameters deviated in a tiny amount from the  $(0, 0)$ . Technically, given the targeted parameters  $(\alpha_S, \beta_M)$ , we construct local parameters  $\alpha_{S,n} \stackrel{\text{def}}{=} \alpha_S + n^{-1/2}b_{\alpha_S}$  and  $\beta_{M,n} \stackrel{\text{def}}{=} \beta_M + n^{-1/2}b_{\beta_M}$ , where  $b_{\alpha_S} > 0$  and  $b_{\beta_M} > 0$  are given constants. Consequently, a generalized SEM may be formed in light of the following local covariance structure:

$$\Gamma_n = (\mathbf{I} - \Theta_n)^{-1}(\mathbf{I} - \Theta_n)^{-\top}, \quad \text{with } \Theta_n = \text{LT}(\alpha_{S,n}, \gamma_S, \beta_{M,n}). \quad (3.1)$$

The utility of  $n^{-1/2}$ -vicinity of local neighboring values  $(\alpha_{S,n}, \beta_{M,n})$  is technical by appealing to proceed theoretical investigation of local asymptotic behaviors in order to test the null hypothesis (2.4). This type technique has also been used by Wang et al. (2018b) and He et al. (2023).

To proceed, we assume some regularity conditions that are widely used in the literature of M estimation and bootstrap to ensure both consistency and asymptotic normality (van der Vaart, 1998).

*Condition 3.* Let  $\theta_0 \stackrel{\text{def}}{=} (\alpha_S, \beta_M, \gamma_S, \zeta_S^\top, \zeta_M^\top, \zeta_Y^\top, \phi_S, \phi_M, \phi_Y)^\top \in \mathbb{R}^{3p+6}$  be the true parameters. Denote the log likelihood by  $\ell_n(\theta) \stackrel{\text{def}}{=} 1/n \sum_{i=1}^n \ell_\theta(S_i, M_i, Y_i, X_i)$ . Assume that the parameter space  $\Theta_0 \subset \mathbb{R}^{3p+6}$  that  $\theta_0$  resides is open and compact. Let  $\epsilon > 0$ . (i) The log-likelihood function  $\ell_\theta$  is twice continuously differentiable almost surely and dominated by certain integrable function. (ii) In a neighbor of  $\theta_0$ ,  $\ell_\theta$  is Lipschitz continuous regarding  $\theta$  with a Lipschitz constant  $L(s, m, y, x)$  that has a finite  $(2 + \epsilon)$ th moment. (iii) The score function  $\nabla_\theta \ell_\theta$  is dominated by a function whose  $(2 + \epsilon)$ th moment is finite. (iv) The variability matrix  $\text{E}(\nabla_\theta^2 \ell_\theta)$  exists and is nonsingular at point  $\theta_0$ .

**THEOREM 2.** *Assume Conditions 1 to 3 hold. Consider the null hypothesis  $H_0$  in the generalized SEM in (3.1). We have*

(i) when  $(\alpha_S, \beta_M) \neq (0, 0)$ ,

$$n^{1/2}\{\widehat{\text{qNIE}}_\tau(s, s'; x) - \text{qNIE}_\tau(s, s'; x)\} \xrightarrow{d} \eta_\tau(x)(\alpha_S Z_2 + Z_1 \beta_M)(z_{s'} - z_s)/\delta_Y;$$

(ii) when  $(\alpha_S, \beta_M) = (0, 0)$ ,

$$n\{\widehat{\text{qNIE}}_\tau(s, s'; x) - \text{qNIE}_\tau(s, s'; x)\} \xrightarrow{d} \eta_\tau(x)(Z_1 Z_2 + Z_1 b_\beta + b_\alpha Z_2)(z_{s'} - z_s)/\delta_Y,$$

where  $Z_1$  and  $Z_2$  are random variables with the same limiting distributions of  $n^{1/2}(\widehat{\alpha}_S - \alpha_S)$  and  $n^{1/2}(\widehat{\beta}_M - \beta_M)$ , respectively, and

$$\eta_\tau(x) = \frac{\phi\{q_\tau(x)\}}{f_{Y|X}(Q_{Y|X}[\Phi\{q_\tau(x)\}])}, \quad q_\tau(x) = \frac{\{\gamma_S z_{s'} + \Phi^{-1}(\tau)(1 + \beta_M^2)^{1/2}\}}{\delta_Y},$$

$z_s = z_s(x) = \Phi^{-1}\{F_{S|X}(s | x)\}$ ,  $\delta_Y = (\eta^2 + \beta_M^2 + 1)^{1/2}$ , and  $\phi(\cdot)$  is the probability density function of standard normal distribution.

Theorem 2 suggests that the difference  $\widehat{\text{qNIE}}_\tau(s, s'; x) - \text{qNIE}_\tau(s, s'; x)$  has a non-uniform limiting distribution with regards to  $(\alpha_S, \beta_M)$ . This non-uniformity occurs for  $(\alpha_S, \beta_M) = (0, 0)$



or  $\neq 0$ ; they have different convergence rates, which will be used in Section 3.2 to isolate  $\Omega_{0,3}$  via a pretest procedure. It is interesting to note that in the vicinity of  $(\alpha_S, \beta_M) = (0, 0)$ , the limiting distribution of  $n\{\widehat{\text{qNIE}}_\tau(s, s'; x) - \text{qNIE}_\tau(s, s'; x)\}$  is continuously scaled by  $(b_\alpha, b_\beta)$ . Such local limit allows us to increase the accuracy of the finite-sample behaviors compared to the classical nonparametric bootstrap method, that ignores the local asymptotic patterns.

### 3.2. Adaptive bootstrap test

Separating the “troublemaker”  $\Omega_{0,3}$  from the other two subspaces  $\Omega_{0,1}$  and  $\Omega_{0,2}$  is feasible due to the different convergence rates in Theorem 2, which can be done by comparing the absolute values of  $\widehat{T}_{\alpha_S} = n^{1/2}\widehat{\alpha}_S/\widehat{\sigma}_{\alpha_S}$  and  $\widehat{T}_{\beta_M} = n^{1/2}\widehat{\beta}_M/\widehat{\sigma}_{\beta_M}$  to certain thresholds. Here,  $\widehat{\sigma}_{\alpha_S}$  and  $\widehat{\sigma}_{\beta_M}$  represent any consistent estimates for the population variances  $\sigma_{\alpha_S}$  and  $\sigma_{\beta_M}$ , respectively. We propose the following “mixture” quantity:

$$\begin{aligned} \widehat{\text{qNIE}}_\tau(s, s'; x) - \text{qNIE}_\tau(s, s'; x) &= \{\widehat{\text{qNIE}}_\tau(s, s'; x) - \text{qNIE}_\tau(s, s'; x)\} \times (1 - I_{\alpha_S, \lambda_n} I_{\beta_M, \lambda_n}) \\ &\quad + \{\widehat{\text{qNIE}}_\tau(s, s'; x) - \text{qNIE}_\tau(s, s'; x)\} \times I_{\alpha_S, \lambda_n} I_{\beta_M, \lambda_n}, \end{aligned} \quad (3.2)$$

where  $I_{\alpha_S, \lambda_n} = I(|\widehat{T}_{\alpha_S, n}| \leq \lambda_n, \alpha_S = 0)$  and  $I_{\beta_M, \lambda_n} = I(|\widehat{T}_{\beta_M, n}| \leq \lambda_n, \beta_M = 0)$  are two flags for the null subspaces, and  $I(\cdot)$  is the usual indicator function. Clearly, when  $(\alpha_S, \beta_M) \neq (0, 0)$ , the classical bootstrap is consistent for the first term in (3.2), while for the second term, Theorem 2 navigates us to construct a consistent bootstrap procedure.

As usual, a superscript  $*$  indicates nonparametric bootstrap. When  $(\alpha_S, \beta_M) = (0, 0)$ , following the limit Theorem 2 (ii), we may construct a bootstrap statistic  $\mathbb{R}_n^*(b_\alpha, b_\beta)$  as a bootstrap counterpart of  $\eta_\tau(x)(Z_1 Z_2 + Z_1 b_\beta + b_\alpha Z_2)(z_{s'} - z_s)/\delta_Y$ . That is,

$$\mathbb{R}_n^*(b_\alpha, b_\beta) = \{Z_1^* Z_2^* (\widehat{z}_{s'}^* - \widehat{z}_s^*) + Z_1^* b_\beta (\widehat{z}_{s'}^* - \widehat{z}_s^*) + b_\alpha Z_2^* (\widehat{z}_{s'}^* - \widehat{z}_s^*)\} \widehat{\eta}_\tau^*(x) / \widehat{\delta}_Y^*,$$

where  $\widehat{z}_s^* = \Phi^{-1}\{\widehat{F}_{S|X}^*(s | x)\}$ ,  $\widehat{\delta}_Y^* = \{(\widehat{\gamma}_S^* + \widehat{\alpha}_S^* \widehat{\beta}_M^*)^2 + (\widehat{\beta}_M^*)^2 + 1\}^{1/2}$ ,  $\widehat{\eta}_\tau^*(x) = \phi\{\widehat{q}^*(x)\} / \widehat{f}_{Y|X}^*(\widehat{Q}_{Y|X}^*[\Phi\{\widehat{q}^*(x)\}])$  with  $\widehat{q}^*(x) = \{\gamma_S^* \widehat{z}_{s'}^* + \Phi^{-1}(\tau)\} / \widehat{\delta}_Y^*$ , and  $Z_1^*$  and  $Z_2^*$  are the usual nonparametric bootstrap counterparts of  $Z_1$  and  $Z_2$ . In our case, since  $Z_1$  and  $Z_2$  are two limiting variables of  $n^{1/2}\widehat{\alpha}_S$  and  $n^{1/2}\widehat{\beta}_M$ , we propose  $Z_1^*$  and  $Z_2^*$  as  $n^{1/2}\widehat{\alpha}_S^*$  and  $n^{1/2}\widehat{\beta}_M^*$ . When  $(\alpha_S, \beta_M) \neq (0, 0)$ , we remain using the classical nonparametric bootstrap estimate  $\widehat{\text{qNIE}}_\tau^*(s, s'; x)$ .

In our AB test, flags  $I_{\alpha_S, \lambda_n}$  and  $I_{\beta_M, \lambda_n}$  are replaced by their bootstrap counterparts of the forms:

$$I_{\alpha_S, \lambda_n}^* = I(|\widehat{T}_{\alpha_S}^*| \leq \lambda_n, |\widehat{T}_{\alpha_S}| \leq \lambda_n), \quad I_{\beta_M, \lambda_n}^* = I(|\widehat{T}_{\beta_M}^*| \leq \lambda_n, |\widehat{T}_{\beta_M}| \leq \lambda_n),$$

where  $\widehat{T}_{\alpha_S}^* = n^{1/2}\widehat{\alpha}_S^*/\widehat{\sigma}_{\alpha_S}^*$  and  $\widehat{T}_{\beta_M}^* = n^{1/2}\widehat{\beta}_M^*/\widehat{\sigma}_{\beta_M}^*$  denote the bootstrap versions of  $\widehat{T}_{\alpha_S} = n^{1/2}\widehat{\alpha}_S/\widehat{\sigma}_{\alpha_S}$  and  $\widehat{T}_{\beta_M} = n^{1/2}\widehat{\beta}_M/\widehat{\sigma}_{\beta_M}$ . Here, we use sample standard deviation estimates based on  $\{n^{1/2}\widehat{\alpha}_S^*\}$  and  $\{n^{1/2}\widehat{\beta}_M^*\}$  for  $\widehat{\sigma}_{\alpha_S}^*$  and  $\widehat{\sigma}_{\beta_M}^*$ , respectively. Thus, following (3.2), we propose an AB test statistic,

$$U_\tau^* = \{\widehat{\text{qNIE}}_\tau^*(s, s'; x) - \widehat{\text{qNIE}}_\tau(s, s'; x)\} \times (1 - I_{\alpha_S, \lambda_n}^* I_{\beta_M, \lambda_n}^*) + n^{-1} \mathbb{R}_n^*(b_\alpha, b_\beta) \times I_{\alpha_S, \lambda_n}^* I_{\beta_M, \lambda_n}^*.$$

We establish the bootstrap consistency of  $U_\tau^*$ .

**THEOREM 3.** *Assume Conditions 1 to 3. Under the generalized SEM (3.1), if the tuning parameter  $\lambda_n$  satisfies  $\lambda_n = o(n^{1/2})$  and  $\lambda_n \rightarrow \infty$  as  $n \rightarrow \infty$ ,  $c_n U_\tau^* \xrightarrow{d} c_n \{\widehat{\text{qNIE}}_\tau(s, s'; x) - \text{qNIE}_\tau(s, s'; x)\}$ , where  $c_n$  is a non-random scaling factor satisfying  $c_n = n^{1/2} \cdot I\{(\alpha_S, \beta_M) \neq (0, 0)\} + n \cdot I\{(\alpha_S, \beta_M) = (0, 0)\}$ .*

Theorem 3 indicates that the AB statistic  $U_\tau^*$  is a consistent bootstrap estimate for the discrepancy  $\widehat{\text{qNIE}}_\tau(s, s'; x) - \text{qNIE}_\tau(s, s'; x)$  under the null model with  $(b_\alpha, b_\beta) = (0, 0)$ , if appropriately scaled. Additionally, for a fixed target parameter  $(\alpha_S, \beta_M)$ , in their neighborhoods, i.e.,  $(b_\alpha, b_\beta) \neq (0, 0)$ , the bootstrap consistency remains valid as a smooth function of  $(b_\alpha, b_\beta)$ . This suggests that even a small change in the target parameters does not affect the bootstrap consistency in Theorem 3, and the AB test statistic  $U_\tau^*$  behaves desirably under the local alternatives to gain statistical power.

In practice, since  $\alpha_S$  and  $\beta_M$  are unknown, we do not use the scaling factor  $c_n$  but directly use  $U_\tau^*$  as the bootstrap statistic for  $\widehat{\text{qNIE}}_\tau(s, s'; x) - \text{qNIE}_\tau(s, s'; x)$ . The rationale is that using  $n^{1/2}U_\tau^*$  to bootstrap  $n^{1/2}\{\widehat{\text{qNIE}}_\tau(s, s'; x) - \text{qNIE}_\tau(s, s'; x)\}$  under  $\Omega_{0,1}$  or  $\Omega_{0,2}$  is equivalent to using  $nU_\tau^*$  to bootstrap  $n\{\widehat{\text{qNIE}}_\tau(s, s'; x) - \text{qNIE}_\tau(s, s'; x)\}$  under  $\Omega_{0,3}$ . Therefore, the distribution of  $U_\tau^*$  will approximate that of  $\widehat{\text{qNIE}}_\tau(s, s'; x) - \text{qNIE}_\tau(s, s'; x)$  regardless of the underlying true null case, as desired.

### 3.3. Implementation of AB test

Given a nominal level denoted by  $\omega$ , we calculate the upper and lower  $\omega/2$  quantiles of the bootstrap statistics  $U_\tau^*$ , denoted by  $q_{1-\omega/2}$  and  $q_{\omega/2}$ , respectively. If estimate  $\widehat{\text{qNIE}}_\tau(s, s'; x)$  falls outside the interval  $(q_{\omega/2}, q_{1-\omega/2})$ , we reject the null hypothesis and conclude that the quantile mediation effect is statistically significant at the level  $\omega$ . It is worth reiterating that the primary goal is to test  $H_0$  with the true underlying  $\alpha_S$  and  $\beta_M$ . The strategy of creating  $n^{1/2}$ -local parameters  $(\alpha_{S,n}, \beta_{M,n})$  is to investigate local asymptotic behaviors. Therefore, to test the null in (2.4) under the null model, we only need to calculate  $U_\tau^*$  with  $b_{\alpha_S} = b_{\beta_M} = 0$ .

### 3.4. Choice of the tuning parameter $\lambda_n$

To apply Theorem 3, we need to ensure  $\lambda_n = o(n^{1/2})$  and increases to infinity as  $n$  approaches infinity. Under this condition, the proposed thresholding method provides a consistent pretest for  $\alpha_S = 0$  and  $\beta_M = 0$  with an asymptotically negligible Type I error rate, i.e.,  $\text{pr}(|\widehat{T}_{\alpha_S}| > \lambda_n, |\widehat{T}_{\beta_M}| > \lambda_n \mid \alpha_S = \beta_M = 0) \rightarrow 0$ . In contrast, if  $\lambda_n$  is bounded, the proposed AB test reduces to the traditional bootstrap method, which is known to suffer from inflated Type I error rates. In all our experiments, we chose  $\lambda_n = \lambda n^{1/2}/\log n$  with  $\lambda$  equal to 2, which worked strikingly well in all simulation studies.

### 3.5. Model diagnosis for copula specification

The generalized SEM is specified with the utility of a Gaussian copula for the DAG, under which we establish estimation and hypothesis testing methods. However, the choice of Gaussian copula may be subject to misspecification of the model. To confirm this specification of the model, we propose using a goodness of fit (GoF) test developed by Zhang et al. (2016). The central idea of the GoF test involves comparing the ‘‘in-sample’’ and ‘‘out-of-sample’’ pseudo-likelihoods. Applying this GoF test in our empirical study of the analysis of metabolic data on childhood obesity, as detailed in Figure 6 of Section 5, we showed that there exists little evidence in the data against the use of Gaussian copula in the specification of the generalized SEM. In effect, the modeling of DAG on the rank-based dependence is rather powerful to capture nonlinear dependencies in our data and beyond; see, e.g., Zhang et al. (2022).

## 4. SIMULATION STUDIES

## 4.1. Setup

In this section, we conduct experiments to examine the finite-sample performance of our proposed method. The data are generated from the generalized SEM (2.1). Marginally,  $S | X \sim \mathcal{N}(X^\top \zeta_S, \sigma_S^2)$ ,  $M | X \sim \mathcal{N}(X^\top \zeta_M, \sigma_M^2)$ , and  $Y | X \sim \text{Exp}\{\exp(X^\top \zeta_Y)\}$ . Set  $\zeta_S = (0.5, 0.2, 0.2, 0)^\top$ ,  $\zeta_M = (0.8, 0.3, 0.3, 0.4)^\top$ , and  $\zeta_Y = (-0.2, 0.4, -0.2, 0.7)^\top$ , and  $\sigma_S = \sigma_M = 0.3$ . Write  $X = (1, X_2, X_3, X_4)^\top$  and  $(X_2, X_3, X_4)^\top \sim \mathcal{N}\{\mathbf{0}, 0.3^2 \text{CS}(0.2)\}$ , where  $\text{CS}(0.2)$  is a compound symmetry matrix with correlation 0.2. Throughout, we vary sample size  $n \in \{300, 500\}$ , set the bootstrap sample size at 500, and set always  $\gamma_S = 0.5$ . We report simulation results under  $n = 300$  in the main text; the additional simulation results under  $n = 500$  are similar and included in Section G of the Supplementary Material. We examine the qNIE with  $s = 0$ ,  $s' = 1$  and  $X = (1, 0, 0, 0)^\top$ . We focus on the median quantile level  $\tau = 0.5$  in all simulations.

We compare our method (QMA-AB) with five competitors: (a) the naive nonparametric bootstrap for the quantile mediation effect test (QMA-B); (b) the classical nonparametric bootstrap for the PoC test (Bind et al., 2017, PoC-B); (c) a generalized Sobel's test (Yuan & MacKinnon, 2014, PoC-YM); (d) the classical nonparametric bootstrap for the joint significance test (Yuan & MacKinnon, 2014, JS-B); (e) a generalized joint significance test (Yuan & MacKinnon, 2014, JS-YM).

## 4.2. Effect of sample size and structural parameters on estimation

In this subsection, we investigate the impact of sample size and structural parameters on estimating  $\text{qNIE}_\tau$  and  $\text{qNDE}_\tau$ . The sample size  $n$  varies over  $\{200, 400, 600, 800, 1000\}$ , while the structural parameters  $(\alpha_S, \beta_M)$  are selected from different combinations in  $\{0, 0.5, 0.5\}$ . The mean squared error (MSE), along with the ratio of MSE relative to the MSE for  $n = 200$ , is summarized in Table 1. The simulation results reveal distinct convergence rates, consistent with our theoretical findings in Theorem 2. Notably, the MSE for  $\text{qNIE}_\tau$  decreases quadratically as the sample size increases when  $(\alpha_S, \beta_M) = (0, 0)$ , and decreases linearly for other parameter combinations.

Table 1: Mean squared error (MSE) of  $\text{qNIE}_\tau$  and  $\text{qNDE}_\tau$  across different combinations of  $(\alpha_S, \beta_M)$  for varying sample sizes  $n \in \{200, 400, 600, 800, 1000\}$ . The table also presents the ratio of MSE relative to the MSE at  $n = 200$ . The quantile level is fixed at  $\tau = 0.5$ , and  $\gamma_S = 0.5$ .

$(\alpha_S, \beta_M)$	$n$	200	400	600	800	1000	Ratio of MSE			
		MSE					400	600	800	1000
(0, 0)	$\text{qNIE}_\tau$	0.26	0.07	0.03	0.02	0.01	3.59	8.61	14.74	22.56
	$\text{qNDE}_\tau$	21.15	10.48	6.76	5.11	4.33	2.02	3.13	4.14	4.88
(0.5, 0)	$\text{qNIE}_\tau$	14.77	7.05	4.55	3.44	2.75	2.10	3.25	4.29	5.36
	$\text{qNDE}_\tau$	34.41	16.94	11.43	8.49	7.00	2.03	3.01	4.06	4.91
(0, 0.5)	$\text{qNIE}_\tau$	11.46	6.13	3.73	2.88	2.34	1.87	3.07	3.98	4.91
	$\text{qNDE}_\tau$	15.56	7.90	5.43	3.89	3.17	1.97	2.87	3.99	4.91
(0.5, 0.5)	$\text{qNIE}_\tau$	11.46	6.13	3.73	2.88	2.34	1.87	3.07	3.98	4.91
	$\text{qNDE}_\tau$	15.56	7.90	5.43	3.89	3.17	1.97	2.87	3.99	4.91

## 4.3. Type I error rate

*Setting I: A fixed null.* In the setting of fixed null, we examine the distributions of the  $p$ -values of six tests over 2000 replications under each of the following three fixed null hypotheses with  $H_{\Omega_{0,1}} : (\alpha_S, \beta_M) = (0.5, 0)$ ,  $H_{\Omega_{0,2}} : (\alpha_S, \beta_M) = (0, 0.5)$ , and  $H_{\Omega_{0,3}} : (\alpha_S, \beta_M) = (0, 0)$ . Figure 3 shows Q-Q plots, which are expected to be uniformly distributed when type I error is properly

controlled. It is evident that in the scenarios of  $H_{\Omega_{0,1}}$  and  $H_{\Omega_{0,2}}$ , all tests'  $p$ -value distributions are approximately uniformly distributed over  $(0, 1)$  except for PoC-B and PoC-YM, due to the violation of the linearity and/or normality assumptions by these two tests under the generalized SEM. It is interesting to note that none of the competing methods, including the naive nonparametric bootstrap test QMA-B can properly control the type I error under  $\Omega_{0,3}$ . Unfortunately, this is the method that has been taken for granted in practice. Our proposed method is the only AB test that produces uniformly distributed  $p$ -values under all three cases. This desirable type I error control leads to power gain as seen in Section 4.4.

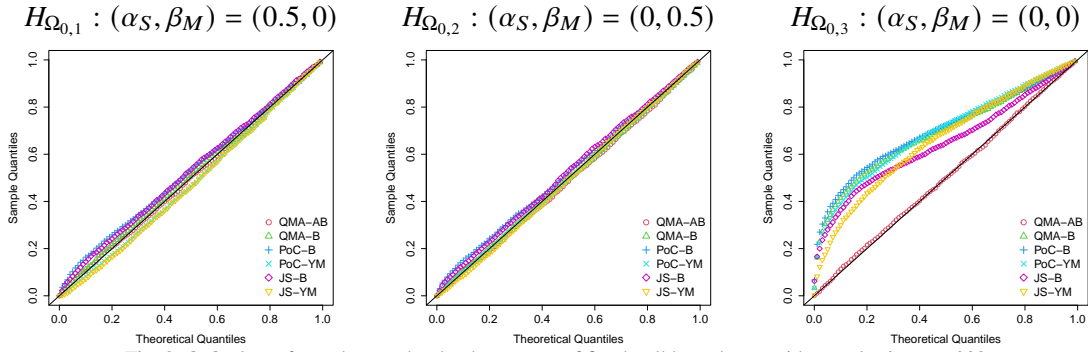


Fig. 3: Q-Q plots of  $p$ -values under the three cases of fixed null hypotheses with sample size  $n = 300$ .

*Setting II: A mixture of nulls.* In this simulation design, we vary the configuration of the null hypotheses. That is, at each replication, a null is randomly drawn from  $H_{\Omega_{0,1}}$ ,  $H_{\Omega_{0,2}}$  and  $H_{\Omega_{0,3}}$  defined above in Setting I. We consider three selection probabilities: (A)  $(1/3, 1/3, 1/3)$ , (B)  $(0.2, 0.2, 0.6)$ , and (C)  $(0.05, 0.05, 0.9)$ , in which the proportion of  $\Omega_{0,3}$  increases from scenario (A) to scenario (C). This design mimics real-world applications where the test is repeatedly used for a large number of mediators that may have different mediation pathways. Figure 4 displays Q-Q plots of  $p$ -values under these three selection probabilities for non-fixed null hypotheses.

Interestingly, our proposed AB test performs steadily well under all the settings, giving rise to high confidence of the methodology to be used in practice. It is easy to visualize that all five competing tests exhibit excessive conservatism in all scenarios (A)-(C), and become increasingly conservative as the proportion of  $\Omega_{0,3}$  increases. Arguably, this may pose a concern in biological studies with many mediators, especially where null subspace  $\Omega_{0,3}$  predominates the configuration of null cases. Therefore, our AB test may enhance scientific discoveries with proper type I error control and desirable power.

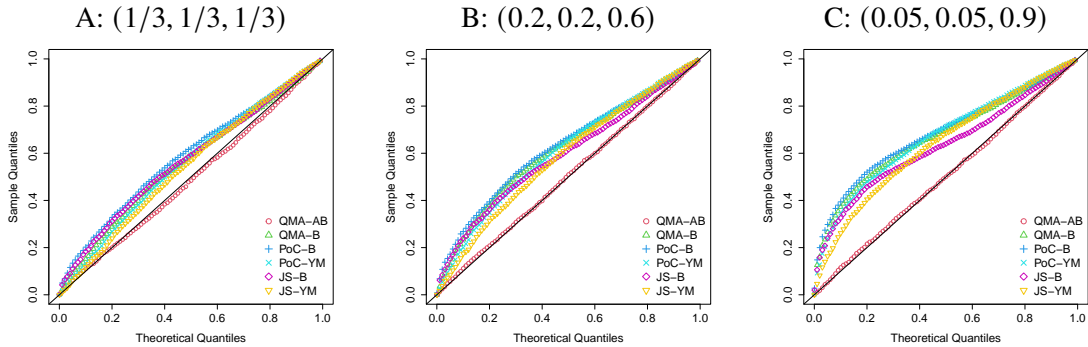


Fig. 4: Q-Q plots of  $p$ -values under the non-fixed null hypotheses with these selection probabilities and sample size  $n = 300$ .

## 4.4. Power evaluation

We assess the statistical power of our proposed AB test in two settings: (i)  $\alpha_S = \beta_M$  that gradually increases from 0 to 0.2, and (ii)  $\alpha_S\beta_M = 0.2^2$  with varying ratio of  $\alpha_S/\beta_M$ . In Figure 5, we present the empirical rejection rates over 2000 replications against the signal size  $\alpha_S$  (the left panel) and the ratio (the right panel), respectively. With no surprise, the best type I error control gives the highest return for the statistical power, justified by the evidence that our QMA-AB exhibits the largest power curves than the five competing methods.

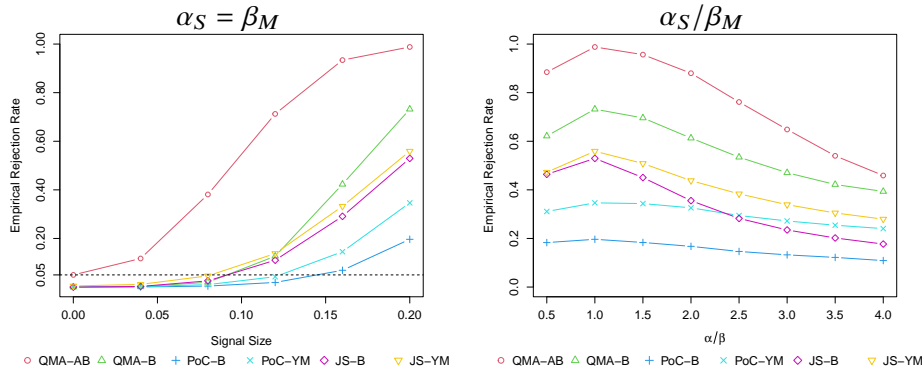


Fig. 5: Empirical rejection rate of the six tests over signal strength of the mediation pathway.

## 5. CHILDHOOD OBESITY METABOLIC STUDY

We apply our proposed methodology to analyze a dataset collected from the ELEMENT cohort study (Perng et al., 2019). The dataset comprises 291 adolescents aged 10–18 years from Mexico City. The pressing need for potential intervention options against the early onset of obesity has drawn significant attention to environmental toxicants, such as phthalates, which have been identified as ubiquitous risk factors for childhood obesity (Yang et al., 2017). Our data analysis aims to identify potential mediation pathways in that metabolites, particularly lipids, may mediate the association of exposure to toxicants with childhood obesity. Molecular-level alterations in metabolic profiles triggered by certain toxicants may facilitate the discovery of important mediation pathways associated with early onset of obesity.

We focus on a target toxicant, maternal phthalate MEOHP, measured in the 3rd trimester of pregnancy, a ubiquitous chemical existing in food production and storage. Childhood obesity, defined by a BMI at or above the 95th percentile for children and teens of the same age and sex (Centers for Disease Control and Prevention, 2022), points to the choice of  $\tau = 0.95$  in our analysis. We focus on 158 lipid metabolites as potential mediators, and aim to identify important mediation pathways of MEOHP  $\rightarrow$  lipid  $\rightarrow$  childhood obesity at the quantile level  $\tau = 0.95$ . Eight potential confounders are included: mother’s age at delivery, birth weight, number of pregnancies, gestational age, education, marital status, and child’s age and sex. Following the literature, we transform MEOHP using the square root, and lipids are all transformed into z-scores in the analysis. According to Juvanhol et al. (2016), BMI is modeled by a Gamma distribution in the generalized SEM.

We apply six methods that have been compared in the simulation studies: QMA-AB, QMA-B, PoC-B, PoC-YM, JS-B, and JS-YM, with 2000 bootstrap samples. For ease of interpretation, we set reference confounders as girl of 16.38 years with a birth weight of 3.13 kg, a gestational age of 38.73 weeks, whose mothers are married, aged 26.85 years old, have received 10.78 years of

education, and have had 2 pregnancies. Exposure to MEOHP changes from zero (no exposure) to a one-unit increase (i.e.,  $s = 0$  to  $s' = 1$ ).

First, we assess the overall set-level significance of the 158 lipids using the Cauchy combination test (Liu & Xie, 2020), and find  $p$ -values equal to 0.0375 (QMA-AB), 0.7339 (QMA-B), 0.8029 (PoC-B), 0.8722 (PoC-YM), 0.7805 (JS-B), and 0.3574 (JS-YM). Of note, only our AB test detected the overall statistical significance for the mediation pathway MEOHP  $\rightarrow$  lipid set  $\rightarrow$  childhood obesity, where the other five methods fail to detect any signals.

Second, we examine individual-level pathways, one lipid at a time. Significant pathways are selected based on  $p$ -values obtained by QMA-AB, adjusting for multiple comparisons with a controlled false discovery rate (FDR) at level 0.1 (Benjamini & Hochberg, 1995). We identify seven significant lipids that are significant mediators for the pathway of MEOHP  $\rightarrow$  lipid  $\rightarrow$  childhood obesity; see Table 2. The estimates of qNDE, qTE,  $\alpha_S$ ,  $\beta_M$  and  $\gamma_S$  are listed in Table G.1 of the Supplementary Material.

Table 2: Seven significant lipids found in the quantile mediation analysis of MEOHP  $\rightarrow$  lipid  $\rightarrow$  childhood obesity at controlled FDR rate of 0.1.

Lipid	qNIE <sub>0.95</sub>	$p$ -value					
		QMA-AB	QMA-B	PoC-B	PoC-YM	JS-B	JS-YM
MG 14:0	-0.3168	0.0010	0.0880	0.4095	0.3475	0.7015	0.3054
PC 38:2/PE 41:2	-0.3438	0.0020	0.0955	0.1130	0.0833	0.5020	0.0154
FA 26:1 DiC	-0.4475	0.0025	0.1110	0.8985	0.8971	0.8375	0.8946
FA 15:0 DiC	0.4504	0.0025	0.0655	0.7410	0.7170	0.7655	0.7143
PC 34:3/PE 37:3	-0.3803	0.0025	0.1000	0.7835	0.7613	0.8125	0.7592
PC 32:2/PE 35:2	-0.3534	0.0035	0.1360	0.1715	0.0441	0.3445	0.0069
PC 40:4/PE 43:4	-0.3534	0.0040	0.0355	0.0945	0.0116	0.5600	0.0018

The identified lipids offer valuable insights into the intricate metabolic network associated with lipid mediators and their implications for obesity-related pathways. A summary for the topmost signal MG 14:0 in Table 2 is given below, and more details can be found in Section G.3 of the Supplementary Material. Lipid MG 14:0, characterized as a diacylglycerol and a triacylglycerol (TAG) precursor, is responsible for decreasing serum TAG concentration, TAG synthesis, and increasing energy expenditure, potentially reducing fat accumulation (Yuan et al., 2010). Thus, MG 14:0 may be considered as a prospective peripheral target for new anti-obesity therapeutics (Take et al., 2016).

Closing the analysis, we conducted a sensitivity analysis as well as model diagnosis to evaluate both validity of sequential ignorability and goodness-of-fit of the generalized SEM. Our sensitivity analysis follows the procedure proposed by Imai et al. (2010a), Liu et al. (2022) and Hao et al. (2023). First, we take normal inverse transformations for the triplet  $(S, M, Y)$  in the generalized SEM (2.1):  $Z_S = \Phi^{-1}\{F_{S|X}(S | x)\}$ ,  $Z_M = \Phi^{-1}\{F_{M|X}(M | x)\}$  and  $Z_Y = \Phi^{-1}\{F_{Y|X}(Y | x)\}$ . Then, conditioning on  $X = x$ ,  $Z_S \sim \mathcal{N}(0, 1)$ ,  $Z_M | Z_S \sim \mathcal{N}(\alpha_S Z_S, 1)$ , and  $Z_Y | Z_S, Z_M \sim \mathcal{N}(\gamma_S Z_S + \beta_M \delta_M Z_M, 1)$ , where  $\delta_M = (\alpha_S^2 + 1)^{1/2}$ . Let  $\varepsilon_M = Z_M - \alpha_S Z_S$  and  $\varepsilon_Y = Z_Y - \gamma_S Z_S + \beta_M \delta_M Z_M$ . In the generalized SEM, errors  $\varepsilon_M$  and  $\varepsilon_Y$  are independently normally distributed. When the sequential ignorability condition is violated, it is likely that the correlation  $\rho = \text{corr}(\varepsilon_M, \varepsilon_Y) \neq 0$  and *vice versa*. Following Imai et al. (2010a), we hypothetically vary the value of  $\rho$  and compute the corresponding  $\widehat{\text{qNIE}}_{0.95}$ . For each lipid, we compute  $|\rho_b|$ , the breakpoint of  $|\rho|$  such that the estimate  $\widehat{\text{qNIE}}_{0.95} = 0$ . All lipids with  $|\widehat{\text{qNIE}}_{0.95}| > 0.2$  (at  $\rho = 0$ ) are plotted in Figure 6 (a). For the top mediator MG 14:0, Figure 6 (a) indicates that when  $\text{corr}(\varepsilon_M, \varepsilon_Y) > 0.11$  in order for  $\widehat{\text{qNIE}}_{0.95} = 0$ . A simple calculation unveils that the absolute sample correlation for MG 14:0 is 0.0007, which is much smaller than 0.11. This suggests that

our discovery of MG 14:0 seems trustworthy, which holds the ground for certain mild violations from the zero correlation. Similar findings are obtained for the rest mediators. Thus, the sensitivity analysis shows that our analysis for the ELEMENT dataset is trustworthy.

Finally, we conduct model diagnosis on the generalized SEM in the analysis. We adopt the “in-and-out-of-sample” likelihood ratio test proposed by Zhang et al. (2016) to flag potential model misspecification. All  $p$ -values of the test are plotted in Figure 6 (b). At 0.1 FDR, we have identified only two lipids, FA 10:0 and FA 8:0, that fail to pass the goodness-of-fit test. However, these two lipids are not in the pool of significant mediators. Nevertheless, we shall always be cautious when making any conclusions on such mediators in a model-based analysis.

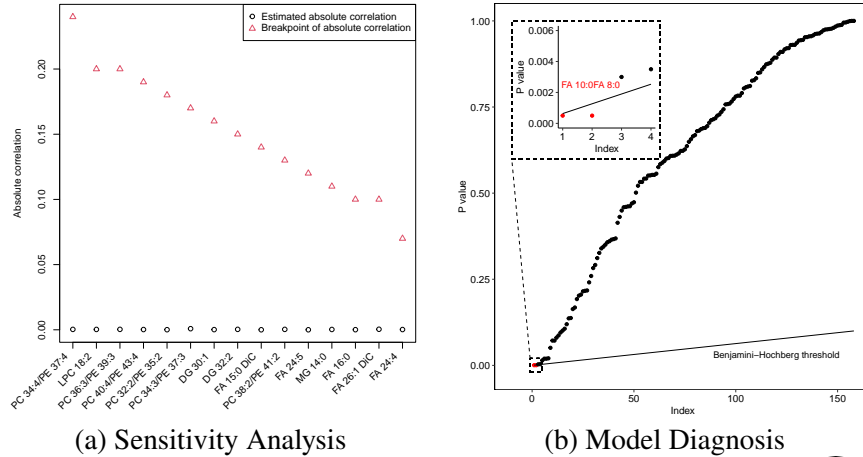


Fig. 6: (a) The estimated breakpoint of the absolute correlation at which  $qNIE_{0.95} = 0$  among lipids whose  $|qNIE_{0.95}| > 0.2$ , and the estimated absolute correlation. (b) The  $p$ -values of the goodness-of-fit test for 158 lipids in ascending order.

## 6. CONCLUDING REMARKS

We developed a new methodology to analyze quantile mediation pathways in the context of generalized SEMs. We discussed in detail both the identification condition and sequential ignorability assumption under which we derived closed-form expressions for quantile mediation estimands. The main technical contribution lies in the development of an adaptive bootstrap procedure that can discern different null subspaces in the construction of test statistics. We have established key theoretical properties, including the bootstrap consistency for the proposed testing method. Extensive simulations have confirmed the theoretical properties, clearly showing that our AB test for the mediation effect has a properly controlled type I error, which leads to significantly improved statistical power over existing methods. One surprise is that only two of 158 lipids may be not modeled by the generalized SEM according to the goodness-of-fit test. This gives the confidence of breadth and flexibility of the generalized SEM.

Our new methodology allows us to consider several important extensions. One is to extend the generalized SEM with the high-dimensional covariates (Guo et al., 2022). In practice, practitioners may include many covariates to increase the chance of making the sequential ignorability assumption a valid condition. The proposed generalized SEM is structured by hierarchical modeling layers that permit the inclusion of high-dimensional covariates in all marginal GLMs. The second extension deals directly with a set of mediators (He et al., 2023; Hao & Song, 2024), rather than the use of Cauchy combination test. Currently, little work has been done for a joint

quantile mediation analysis involving a set of mediators. Flexibility of the generalized SEM may allow us to handle multi-mediators, which is worth further investigation.

#### ACKNOWLEDGEMENT

This research was partially funded by NIH R01ES033565.

#### SUPPLEMENTARY MATERIAL

Supplementary Material includes proofs for all theoretical results in the main text, additional simulation results and interpretations for the identified signals.

#### A. GENERALIZED STRUCTURAL EQUATION MODEL

A DAG, shown in Figure 1 (A), involves three random variables including an exposure  $S \in \mathbb{R}^1$ , a mediator  $M \in \mathbb{R}^1$ , and an outcome  $Y \in \mathbb{R}^1$ . A classical SEM for this DAG takes the form:  $S = \varepsilon_S$ ,  $M = \alpha_S S + \varepsilon_M$ , and  $Y = \beta_M M + \gamma_S S + \varepsilon_Y$ . This gives an algebraic presentation of graphic topology (Pearl, 2014). With the covariance matrix of the three error terms  $(\varepsilon_S, \varepsilon_M, \varepsilon_Y)^T$ ,  $\Sigma \stackrel{\text{def}}{=} \text{diag}(\sigma_{\varepsilon_S}^2, \sigma_{\varepsilon_M}^2, \sigma_{\varepsilon_Y}^2)$ , and the *weighted adjacency matrix*

$$\Theta = \begin{pmatrix} 0 & 0 & 0 \\ \alpha_S & 0 & 0 \\ \gamma_S & \beta_M & 0 \end{pmatrix} \stackrel{\text{def}}{=} \text{LT}(\alpha_S, \gamma_S, \beta_M),$$

clearly, the covariance of  $(S, M, Y)$  is

$$\Gamma \stackrel{\text{def}}{=} \text{var}\{(S, M, Y)^T\} = (\mathbf{I} - \Theta)^{-1} \Sigma (\mathbf{I} - \Theta)^{-T}.$$

Thus parameters  $(\alpha_S, \gamma_S, \beta_M)$  appear solely in the second moment of the joint distribution. As shown in Figure 1 (B), the classical SEM adds confounding factors  $X \in \mathbb{R}^p$  as follows:  $S = \zeta_S^T X + \varepsilon_S$ ,  $M = \alpha_S S + \zeta_M^T X + \varepsilon_M$ , and  $Y = \beta_M M + \gamma_S S + \zeta_Y^T X + \varepsilon_Y$ . The confounding enters the SEM via linear predictors (e.g.  $\zeta_S^T X$ ) that affect only the first moment of the joint distribution; see Section B of the Supplementary Material for details. Such SEM introduces a space perpendicular to  $\text{span}(X)$  so that removal of the linear predictors would have no impact on the DAG topology. That is, the classical SEM suggests that the linear predictors of  $X$  and DAG topology  $\Theta$  reside in two orthogonal spaces. These insights are incorporated into the following extension proposed by Hao et al. (2023) termed generalized SEM.

Hao et al. (2023) suggested incorporating the covariance structure  $\Gamma$  in the Gaussian copula (Song, 2000),  $C(u_1, u_2, u_3) = \Phi_3\{\Phi^{-1}(u_1), \Phi^{-1}(u_2), \Phi^{-1}(u_3); \Gamma'\}$ , where  $\Phi_3(\cdot; \Gamma')$  is a trivariate Gaussian distribution function with mean zero and correlation matrix  $\Gamma'$ , and  $\Phi(\cdot)$  is the standard Gaussian distribution function. In this hierarchical modeling with copula, all the marginal parameters including both regression parameters and variance parameters are included in the marginal distributions, where matrix  $\Gamma = (\mathbf{I} - \Theta)^{-1} (\mathbf{I} - \Theta)^{-T}$  contains only correlation parameters. The resulting joint distribution is expressed as

$$F_{S, M, Y|X}(s, m, y | x) = C\{F_{S|X}(s | x), F_{M|X}(m | x), F_{Y|X}(y | x); \Gamma'\}.$$

Let  $\eta = \alpha_S \beta_M + \gamma_S$  be the total DAG effect. The induced correlation matrix  $\Gamma'$  in the copula joint model has an explicit form:

$$\Gamma' = \begin{pmatrix} 1 & \frac{\alpha_S}{(\alpha_S^2 + 1)^{1/2}} & \frac{\eta}{(\eta^2 + \beta_M^2 + 1)^{1/2}} \\ \frac{\alpha_S}{(\alpha_S^2 + 1)^{1/2}} & 1 & \frac{\alpha_S \eta + \beta_M}{(\alpha_S^2 + 1)^{1/2} (\eta^2 + \beta_M^2 + 1)^{1/2}} \\ \frac{\eta}{(\eta^2 + \beta_M^2 + 1)^{1/2}} & \frac{\alpha_S \eta + \beta_M}{(\alpha_S^2 + 1)^{1/2} (\eta^2 + \beta_M^2 + 1)^{1/2}} & 1 \end{pmatrix}. \quad (\text{A.1})$$

It is interesting to note that the dependence between exposure  $S$  and outcome  $Y$  is  $\text{corr}(S, Y) = \eta / (\eta^2 + \beta_M^2 + 1)^{1/2}$ , a term that contributes to the drift along with a given quantile level in Theorem 1.



*Remark A.1.* The generalized SEM extends the classical linear SEM by allowing non-linear dependence among variables  $(S, M, Y)$ . Because  $\Phi^{-1}\{F(\cdot)\}$  is a non-linear monotone transformation, the correlations in  $\Gamma'$  have close connections with rank-based correlation measures such as Spearman's  $\rho$ , Kendall's  $\tau$ , and Chatterjee's  $\xi$  (Zhang et al., 2022). When  $F$  is normal, the generalized SEM reduces to the classical linear SEM along with Pearson correlation.

We extend the marginal linear regression to the generalized linear model (GLM) for modeling the marginal distributions. Specifically, we assume that given the covariates  $X$ , the marginal distribution of  $S$ ,  $M$ , and  $Y$  are elements of exponential dispersion family distribution (ED) models (Jorgensen, 1987), that is,

$$\begin{aligned} S | X &\sim \text{ED}(\mu_S(X), \phi_S), g_X(\mu_S(X)) = X^T \zeta_S, & M | X &\sim \text{ED}(\mu_M(X), \phi_M), g_M(\mu_M(X)) = X^T \zeta_M \\ Y | X &\sim \text{ED}(\mu_Y(X), \phi_Y), g_Y(\mu_Y(X)) = X^T \zeta_Y, \end{aligned}$$

where  $g_X$ ,  $g_M$  and  $g_Y$  are known link functions, and  $\phi_S$ ,  $\phi_M$  and  $\phi_Y$  are dispersion parameters.

*Remark A.2 (Choice of the marginal distribution).* One can also take other parametric, semiparametric, or fully nonparametric ways to model the marginal distributions. Examples include the linear quantile regression (Wang et al., 2018a), the generalized additive model, and kernel/sieve density regression (Chen, 2007; Imai et al., 2010a). The methodology development in this paper can provide a foundation for valuable generalizations.

#### REFERENCES

- BARON, R. M. & KENNY, D. A. (1986). The moderator–mediator variable distinction in social psychological research: Conceptual, strategic, and statistical considerations. *Journal of Personality and Social Psychology* **51**, 1173–1182.
- BENJAMINI, Y. & HOCHBERG, Y. (1995). Controlling the false discovery rate: A practical and powerful approach to multiple testing. *Journal of the Royal Statistical Society: Series B (Methodological)* **57**, 289–300.
- BIND, M.-A., VANDERWEELE, T. J., SCHWARTZ, J. D. & COULL, B. A. (2017). Quantile causal mediation analysis allowing longitudinal data. *Statistics in Medicine* **36**, 4182–4195.
- CENTERS FOR DISEASE CONTROL AND PREVENTION (2022). About child and teen BMI. <https://bit.ly/49yvvvQ>.
- CHEN, X. (2007). Chapter 76 large sample sieve estimation of semi-nonparametric models. In *Handbook of Econometrics*, vol. 6. Elsevier, pp. 5549–5632.
- DRTON, M. & XIAO, H. (2016). Wald tests of singular hypotheses. *Bernoulli* **22**, 38–59.
- DUFOUR, J.-M., RENAULT, E. & ZINDE-WALSH, V. (2013). Wald tests when restrictions are locally singular. ArXiv:1312.0569.
- FRISCH, R. & WAUGH, F. V. (1933). Partial time regressions as compared with individual trends. *Econometrica* **1**, 387–401.
- GLONEK, G. F. V. (1993). On the behaviour of Wald statistics for the disjunction of two regular hypotheses. *Journal of the Royal Statistical Society: Series B (Methodological)* **55**, 749–755.
- GUO, X., LI, R., LIU, J. & ZENG, M. (2022). High-dimensional mediation analysis for selecting DNA methylation loci mediating childhood trauma and cortisol stress reactivity. *Journal of the American Statistical Association* **117**, 1110–1121.
- HAO, W., CHEN, C. & SONG, P. X.-K. (2023). A class of directed acyclic graphs with mixed data types in mediation analysis. ArXiv:2311.17867.
- HAO, W. & SONG, P. X.-K. (2024). A simultaneous likelihood test for joint mediation effects of multiple mediators. *Statistica Sinica*.
- HE, Y., SONG, P. X. K. & XU, G. (2023). Adaptive bootstrap tests for composite null hypotheses in the mediation pathway analysis. *Journal of the Royal Statistical Society: Series B (Statistical Methodology)* **0**.
- HORVATH, S. (2013). DNA methylation age of human tissues and cell types. *Genome Biology* **14**, R115.
- HSU, Y.-C., HUBER, M. & YEN, Y.-M. (2023). Doubly robust estimation of direct and indirect quantile treatment effects with machine learning. ArXiv:2307.01049.
- HUBER, M., SCHELKER, M. & STRITTMATTER, A. (2022). Direct and indirect effects based on changes-in-changes. *Journal of Business & Economic Statistics* **40**, 432–443.
- IMAI, K., KEELE, L. & TINGLEY, D. (2010a). A general approach to causal mediation analysis. *Psychological Methods* **15**, 309–334.
- IMAI, K., KEELE, L. & YAMAMOTO, T. (2010b). Identification, inference and sensitivity analysis for causal mediation effects. *Statistical Science* **25**, 51–71.

- JOE, H. (2005). Asymptotic efficiency of the two-stage estimation method for copula-based models. *Journal of Multivariate Analysis* **94**, 401–419.
- JORGENSEN, B. (1987). Exponential dispersion models. *Journal of the Royal Statistical Society: Series B (Methodological)* **49**, 127–145.
- JUVANHOL, L. L., LANA, R. M., CABRELLI, R., BASTOS, L. S., NOBRE, A. A., ROTENBERG, L. & GRIEP, R. H. (2016). Factors associated with overweight: Are the conclusions influenced by choice of the regression method? *BMC public health* **16**, 642.
- LI, T., SHI, C., LU, Z., LI, Y. & ZHU, H. (2023). Evaluating Dynamic Conditional Quantile Treatment Effects with Applications in Ridesharing.
- LIU, Y. & XIE, J. (2020). Cauchy combination test: A powerful test with analytic p-value calculation under arbitrary dependency structures. *Journal of the American Statistical Association* **115**, 393–402.
- LIU, Z., SHEN, J., BARFIELD, R., SCHWARTZ, J., BACCARELLI, A. A. & LIN, X. (2022). Large-Scale Hypothesis Testing for Causal Mediation Effects with Applications in Genome-wide Epigenetic Studies. *Journal of the American Statistical Association* **117**, 67–81.
- PEARL, J. (2014). Interpretation and identification of causal mediation. *Psychological Methods* **19**, 459–481.
- PERNG, W., TAMAYO-ORTIZ, M., TANG, L., SÁNCHEZ, B. N., CANTORAL, A., MEEKER, J. D. et al. (2019). Early life exposure in Mexico to environmental toxicants (ELEMENT) project. *BMJ Open* **9**, e030427.
- RUBIN, D. B. (1980). Randomization analysis of experimental data: The Fisher randomization test comment. *Journal of the American Statistical Association* **75**, 591–593.
- SHEN, E., CHOU, C.-P., PENTZ, M. A. & BERHANE, K. (2014). Quantile mediation models: A comparison of methods for assessing mediation across the outcome distribution. *Multivariate Behavioral Research* **49**, 471–485.
- SHPITSER, I. & VANDERWEELE, T. J. (2011). A complete graphical criterion for the adjustment formula in mediation analysis. *The International Journal of Biostatistics* **7**, 16.
- SOBEL, M. E. (1982). Asymptotic confidence intervals for indirect effects in structural equation models. *Sociological Methodology* **13**, 290.
- SONG, P. X.-K. (2000). Multivariate dispersion models generated from Gaussian copula. *Scandinavian Journal of Statistics* **27**, 305–320.
- TAKE, K., MOCHIDA, T., MAKI, T., SATOMI, Y., HIRAYAMA, M., NAKAKARIYA, M. et al. (2016). Pharmacological inhibition of monoacylglycerol o-acyltransferase 2 improves hyperlipidemia, obesity, and Diabetes by change in intestinal fat utilization. *PLoS ONE* **11**, e0150976.
- VAN DER VAART, A. W. (1998). *Asymptotic Statistics*. Cambridge Series in Statistical and Probabilistic Mathematics. Cambridge, UK: Cambridge University Press.
- VANDERWEELE, T. (2015). *Explanation in Causal Inference: Methods for Mediation and Interaction*. New York: Oxford University Press, 1st ed.
- VANDERWEELE, T. J. & VANSTEELENDT, S. (2010). Odds ratios for mediation analysis for a dichotomous outcome. *American Journal of Epidemiology* **172**, 1339–1348.
- WANG, H. J., FENG, X. & DONG, C. (2018a). Copula-based quantile regression for longitudinal data. *Statistica Sinica* **29**, 245–264.
- WANG, H. J., MCKEAGUE, I. W. & QIAN, M. (2018b). Testing for marginal linear effects in quantile regression. *Journal of the Royal Statistical Society. Series B (Statistical Methodology)* **80**, 433–452.
- WANG, W. & YU, P. (2023). Nonequivalence of two least-absolute-deviation estimators for mediation effects. *TEST* **32**, 370–387.
- YANG, T. C., PETERSON, K. E., MEEKER, J. D., SÁNCHEZ, B. N., ZHANG, Z., CANTORAL, A. et al. (2017). Bisphenol a and phthalates in utero and in childhood: Association with child BMI z-score and adiposity. *Environmental Research* **156**, 326–333.
- YUAN, Q., RAMPRASATH, V. R., HARDING, S. V., RIDEOUT, T. C., CHAN, Y.-M. & JONES, P. J. H. (2010). Diacylglycerol oil reduces body fat but does not alter energy or lipid metabolism in overweight, hypertriglyceridemic women. *The Journal of Nutrition* **140**, 1122–1126.
- YUAN, Y. & MACKINNON, D. P. (2014). Robust mediation analysis based on median regression. *Psychological methods* **19**, 1–20.
- ZHANG, S., OKHRIN, O., ZHOU, Q. M. & SONG, P. X. K. (2016). Goodness-of-fit test for specification of semiparametric copula dependence models. *Journal of Econometrics* **193**, 215–233.
- ZHANG, Y., CHEN, C. & ZHU, L. (2022). Sliced independence test. *Statistica Sinica* **32**, 2477–2496.
- ZHOU, Y., SONG, P. X.-K. & WEN, X. (2021). Structural factor equation models for causal network construction via directed acyclic mixed graphs. *Biometrics* **77**, 573–586.

[Received on 2 January 2017. Editorial decision on 1 August 2023]